ELSEVIER

Bioelectrochemistry 56 (2002) 27–32

Bioelectrochemistry

www.elsevier.com/locate/bioelechem

Monolayers of a de novo designed 4-α-helix bundle carboprotein and partial structures on Au(111)-surfaces

Jesper Brask, Hainer Wackerbarth, Knud J. Jensen[1], Jingdong Zhang, Jens U. Nielsen, Jens E.T. Andersen, Jens Ulstrup*

Department of Chemistry, Buildings 201 and 207, Technical University of Denmark, DK-2800 Lyngby, Denmark

Received 1 June 2001; accepted 15 October 2001

Abstract

Mapping of structure and function of proteins adsorbed on solid surfaces is important in many contexts. Electrochemical techniques based on single-crystal metal surfaces and in situ scanning probe microscopies (SPM) have recently opened new perspectives for mapping at the single-molecule level. De novo design of model proteins has evolved in parallel and holds promise for test and control of protein folding and for new tailored protein structural motifs. These two strategies are combined in the present report. We present a synthetic scheme for a new 4-α-helix bundle carboprotein built on a galactopyranoside derivative with a thiol anchor aglycon suitable for surface immobilization on gold. The galactopyranoside with thiol anchor and the thiol anchor alone were prepared for comparison. Voltammetry of the three molecules on Au(111) showed reductive desorption peaks caused by monolayer adsorption via thiolate-Au bonding. In situ STM of the thiol anchor disclosed an ordered adlayer with clear domains and molecular features. This holds promise, broadly for single-molecule voltammetry and the SPM and scanning tunnelling microscopy (STM) of natural and synthetic proteins.

Keywords: 4-α-helix bundle; Carboprotein; De novo design; Single-crystal voltammetry; Au(111)-electrodes; In situ STM

1. Introduction

Structural mapping and electron transfer function of proteins adsorbed on solid surfaces is broadly important [1–3]. Proteins frequently exert their natural function in the adsorbed state, and protein adsorbates can be probed by surface-based techniques such as X-ray photoelectron [3] and resonance Raman spectroscopy [4,5], voltametric methods [6,7], and scanning tunnelling microscopy directly in aqueous solution (in situ STM) [4,8–13].

Protein structure–function relations involve demanding isolation, characterization, and chemical or microbiological modification [1,6,7,12]. De novo design of functional model proteins and development of systematic synthetic procedures have therefore come forward [13–20]. De novo design promises to critically test protein folding and stability, enables construction of 'isolated' structural motifs, and if successful, 'tailor-made' novel protein-like structures. DeGrado et al. [13] studied de novo design of 4-α-helix bundles and other fold targets. Choma et al. [14] and Robertson et al. 15] have developed heme-binding protein models. Mutter and Vuilleumier [16] described cyclic and linear peptides as templates for, especially, 4-α-helix bundles. This template-assembled synthetic protein (TASP) approach was adapted by Rau et al. [17] for the synthesis of metalloprotein models. Two of the present authors have developed the use of monosaccharides as templates for de novo design of 4-α-helix bundles, so-called carboproteins [18–20].

Voltammetry of redox proteins, long established [6,7], has mostly rested on macroscopic voltammetry, and use of polycrystalline electrodes. Mapping of protein surface function towards the molecular level, however, requires well-characterized atomically planar surfaces. This facet of contemporary physical electrochemistry and other facets such as in situ STM have only recently been introduced in the electrochemistry of biological macromolecules [4,10,12,21,22].

Abbreviations: Aoa, aminooxyacetyl; Boc, *tert*-butoxycarbonyl; D-Gal*p*, D-galactopyranose; DIPCDI, *N,N′* -diisopropylcarbodiimide; DMAP, 4-dimethylaminopyridine; HOBt, 1-hydroxybenzotriazole; PyBOP, benzotriazolyloxy-tris-(pyrrolidino) phosphonium hexafluorophosphate; TFA, trifluoroacetic acid; Amino acid symbols denote the L-configuration.

* Corresponding authors. Tel.: +45-45252359; fax: +45-45883136.

E-mail addresses: ju@kemi.dtu.dk (J. Ulstrup), kjj@kemi.kvl.dk (K.J. Jensen).

[1] Tel.: +45 35 28 2730; fax: +45 35 28 2398.

1567-5394/02/$ - see front matter
PII: S1567-5394(02)00055-5

In this report, we describe the synthesis of a novel 4-α-helix bundle carboprotein **1**, which incorporates a thiol anchor from the template. Carboprotein **1** was prepared by oxime ligation of a *C* – terminal peptide aldehyde to a tetra-aminooxyacetyl (Aoa) functionalized D-Gal*p* (galactopyranose) template, similar to a recently described carboprotein [20]. The thiol group allows for adsorption to gold surfaces without interference with folding of the protein. Gal*p* with thiol anchor **2** and thiol anchor **3** were studied for comparison. Voltammetry of the three molecules on Au(111)-electrodes gave reductive desorption of sulfide-bound monolayers. In situ STM of the thiol anchor **3** disclosed an ordered adlayer. These combined strategies show that well-defined layers of the carboprotein **1** and the fragments **2** and **3** form spontaneously, and hold promise for voltammetry of adsorbed redox functionalized 4-α-helix bundle proteins.

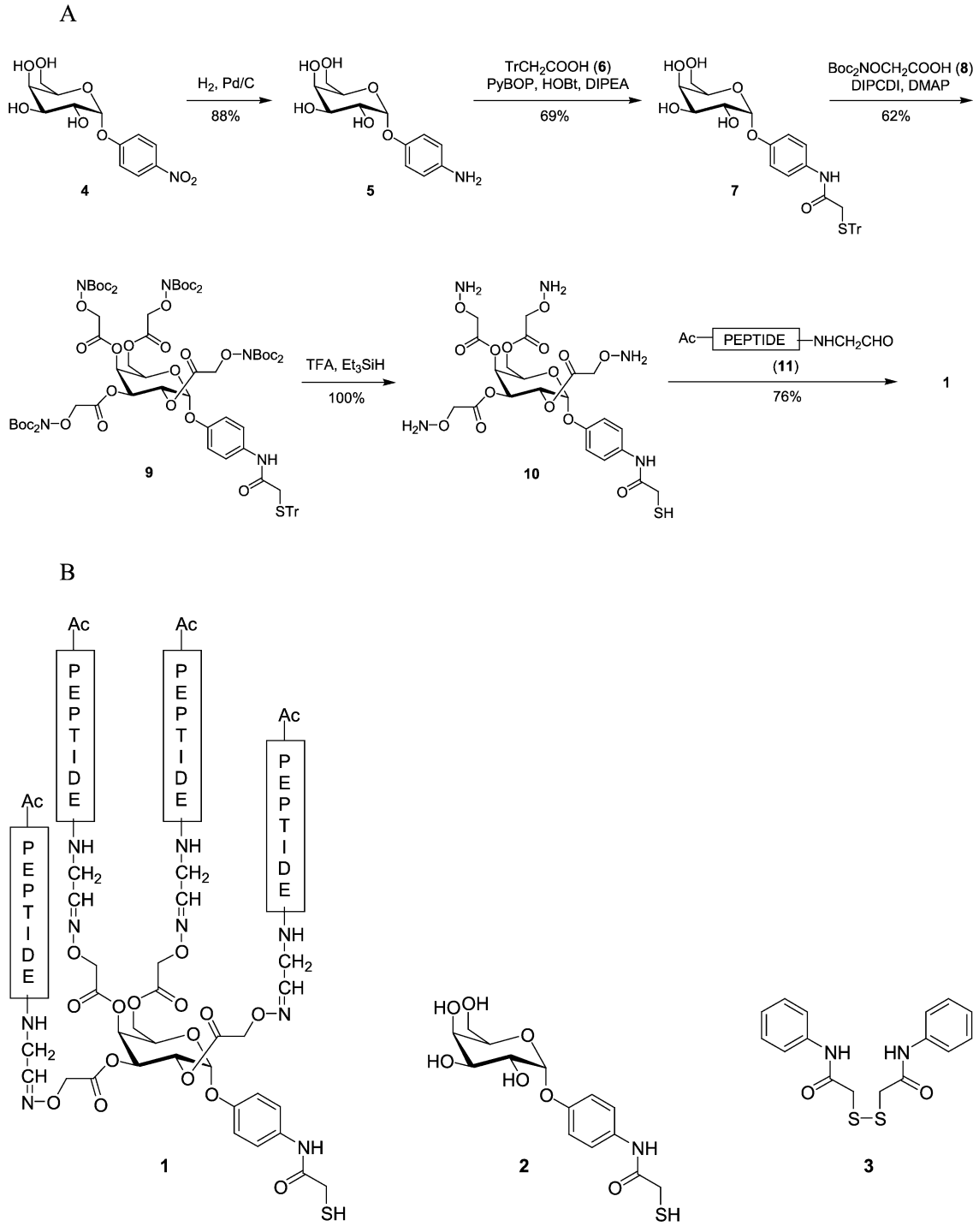

Fig. 1. (A): Synthesis of the 4-α-helix bundle carboprotein **1**. (B): Carboprotein **1**, Gal*p* with thiol anchor **2**, and the thiol anchor disulfide **3**.

2. Experimental

2.1. Reagents and synthesis

Carboprotein **1** was prepared starting from commercially available 4-nitrophenyl α-D-Gal*p* (**4**), which was reduced to the amine **5** in 88% yield by catalytic hydrogenation (Fig. 1A). Chemoselective coupling of **5** to tritylmercaptoacetic acid (**6**), mediated by PyBOP/HOBt provided 4-(tritylmercaptoacetamido)phenyl α-D-Gal*p* (**7**), in 69% yield. While treatment with TFA–CH_2Cl_2–Et_3SiH (1:1:0.1) gave the reference compound 4-(mercaptoacetamido)phenyl α-D-Gal*p* (**2**), per-*O*-acylation of **7** with N^{β},N^{β}-Boc_2-Aoa-OH (**8**), [19] DIPCDI, and DMAP resulted in 4-(tritylmercaptoacetamido)phenyl 2,3,4,6-tetra-*O*-(Boc_2-Aoa)-α-D-Gal*p* (**9**), in 62% yield. Deprotection with TFA–CH_2Cl_2–Et_3SiH (1:1:0.1) provided the desired template 4-(mercaptoacetamido)phenyl 2,3,4,6-tetra-*O*-Aoa α-D-Gal*p* (**10**), in quantitative yield.

Synthesis of the peptide aldehyde Ac-Glu-Ala-Leu-Glu-Lys-Ala-Leu-Lys-Glu-Ala-Leu-Ala-Lys-Leu-Gly-Gly-H (**11**), is described in Ref. [20]. Oxime ligation proceeded with 50% excess of **11** relative to **10** under inert atmosphere to give carboprotein **1** in 76% yield after purification by preparative HPLC.

N-Phenyl-mercaptoacetamide disulfide (**3**) was prepared by DIPCDI-mediated condensation of aniline and tritylmercaptoacetic acid. Deprotection with TFA in the presence of Et_3SiH, followed by air-oxidation provided **3** in 27% overall yield.

Other reagents including Millipore water (18.2 MΩ, Milli-Q-Housing) were ultrapure grade. Buffer solutions were 0.1 M K_2HPO_4/KH_2PO_4, pH 6.9 and 0.01 M NaOH, pH 11.9.

2.2. Preparation of samples

Au(111) substrates for electrochemistry were prepared by the method of Clavilier et al. [23] and Hamelin [24]. Prior to use, Au(111)-electrodes were annealed in a hydrogen flame, kept for 1 min over a water surface, and then inserted into ultrapure water. Clean electrodes were transferred to solutions of the carboprotein or fragment molecules. Carboprotein **1** was adsorbed by soaking the electrode in 0.23 mM carboprotein in 0.1 M phosphate buffer for 18 h. Molecule **2** was adsorbed from 4 mM solution in water for 18 h, **3** from 15 mM solution in methanol for 4 h. The resulting samples were thoroughly rinsed with millipore water.

2.3. Electrochemical measurements and STM imaging

Glassware was cleaned as reported [3,12]. Electrochemical instrumentation was an Autolab system (Eco Chemie, The Netherlands), controlled by the General System software. Capacitance data were recorded by fixing the frequency at 100 Hz with a modulation amplitude of 5 mV. The Au(111)-electrode was used in the hanging meniscus mode. The electrode system included a coiled bright platinum wire as counter electrode and a saturated calomel (SCE) reference electrode. Electrode potentials are referred to the SCE. Solutions were deoxygenated by purified argon (Chrompack 5N), and an argon atmosphere maintained over the solution.

A PicoSPM instrument (Molecular Imaging, USA) with a bipotentiostat for independent control of substrate and tip potential was used for STM imaging. Electrochemical control was conducted in an in-house built three-electrode cell, using 0.1 M $HClO_4$ electrolyte. The substrate was a Au(111)-disc (MaTeck, 10-mm diameter, 1-mm thick). Reference and counter electrodes were Pt-wires. Tungsten tips were prepared and coated as previously [3]. The

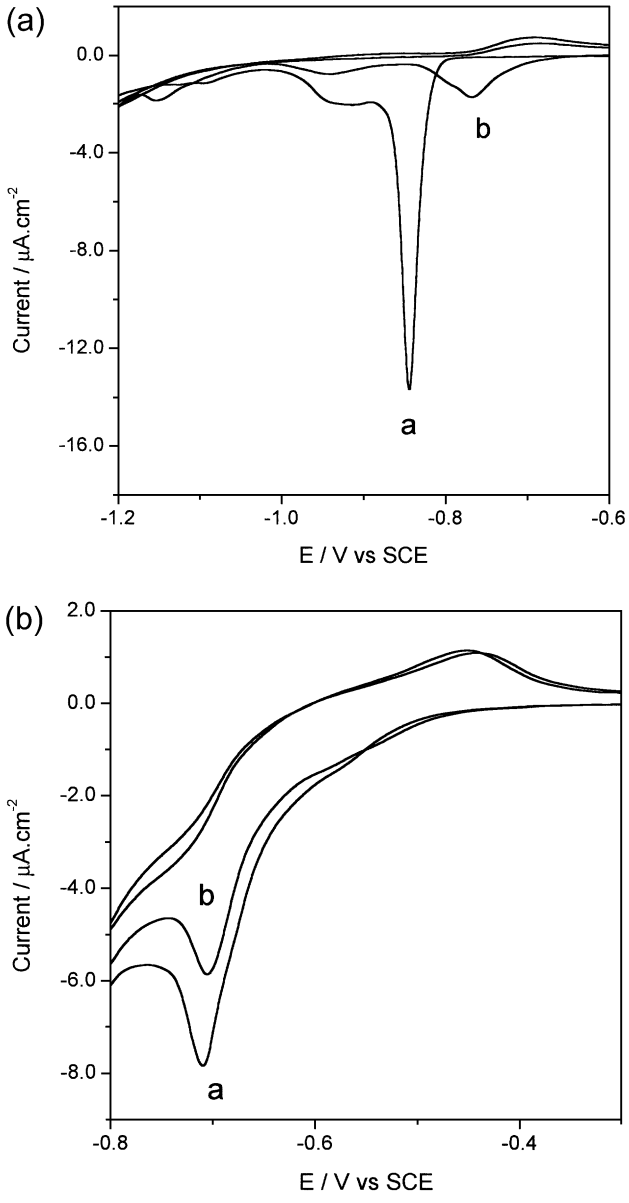

Fig. 2. Reductive desorption of the thiol anchor molecule **3** from Au(111). (a): 10 mM NaOH, pH 11.9; curve a: first scan; curve b: second scan. (b): 0.1 M phosphate buffer, pH 6.9; curve a: first scan; curve b: second scan; scan rate: 10 mV s^{-1}.

Table 1
Peak potentials and adsorbate coverages for reductive desorption of the thiol anchor **3**, the Gal*p* with thiol anchor, **2** and the full carboprotein **1**

	4-α-helix bundle carboprotein **1**		Gal*p* with thiol anchor **2**		Thiol anchor **3**	
	Peak (mV)	Coverage (mol cm^{-2})	Peak (mV)	Coverage (mol cm^{-2})	Peak (mV)	Coverage (mol cm^{-2})
pH = 6.9	− 728	2.0×10^{-11}	− 630	2.4×10^{-10}	−702	2.1×10^{-10}
pH = 11.9	–	–	− 930	3.9×10^{-10}	− 848	5.0×10^{-10}
pH = 11.9/pH = 6.9				1.6		2.4

constant current mode was used with a tip current of 0.3 nA and a bias voltage of 0.2 V.

3. Results and discussion

The synthesis of carboprotein **1** is outlined in Fig. 1A. Synthesis of the carboprotein by oxime formation followed by specific adsorption to a surface, without intermittent deprotection steps, amounts to sequential chemoselective ligation. ESI-MS confirmed the identity of **1** in partially dimerized form via a disulfide bridge (10–20% disulfide). As both the thiol and the disulfide are expected to undergo adsorption, this was not critical.

Fig. 1B shows the structure of the full carboprotein **1**, the Gal*p* with thiol anchor aglycon **2**, and the thiol anchor alone, synthesized as the disulfide **3**. None of the molecules contain a redox group but thiol functionalities adsorb oxidatively on gold surfaces [25,26]. Voltammetric scans to negative potentials reduce the Au–S bond, liberating the thiol-containing molecules. Reductive desorption is commonly characterized by sharp reduction peaks in basic solution. The peak area enables estimation of the molecular coverage, important in STM image interpretation [27].

Fig. 2a shows reductive desorption of the thiol anchor molecule **3** from Au(111) in 10 mM NaOH, pH 11.9. A sharp peak appears at − 848 mV. The small shoulder on the negative side is probably caused by non-ideality of the Au(111)-surface or spurious impurities. A significantly broader peak of about 40% of the peak area in the first scan is seen in the second scan. The positive shift suggests that it is due to re-adsorption of liberated thiol anchor. Reductive desorption in 0.1 M phosphate, pH 6.9 gives a broader peak, at − 702 mV, closer to the onset of dihydrogen evolution (Fig. 2b). This is of interest as reductive desorption distinct from dihydrogen evolution at low pH is not common. The peak area is smaller than at pH 11.9 (Table 1). Subsequent scans show significant but unshifted residual peaks with larger relative areas than at pH 11.9. This suggests that the subsequent peaks are caused by incomplete desorption in the first scan, rather than desorption followed by re-adsorption. Fig. 3a shows reductive desorption of Gal*p* with thiol anchor, **2**, in 10 mM NaOH, pH 11.9. A sharp peak is again observed, shifted negatively to − 930 mV. The hydrophilic carbohydrate group might have been expected to facilitate desorption, shifting the desorption potential positively, and the negative shift could be indicative of lateral intermolecular interactions. As for molecule **3**, a strongly shifted signal is seen in the second scan but much smaller for **2** than for **3**. A broader positively shifted signal at − 630 mV is apparent in phosphate buffer, pH 6.9 (Fig. 3b). This could support that

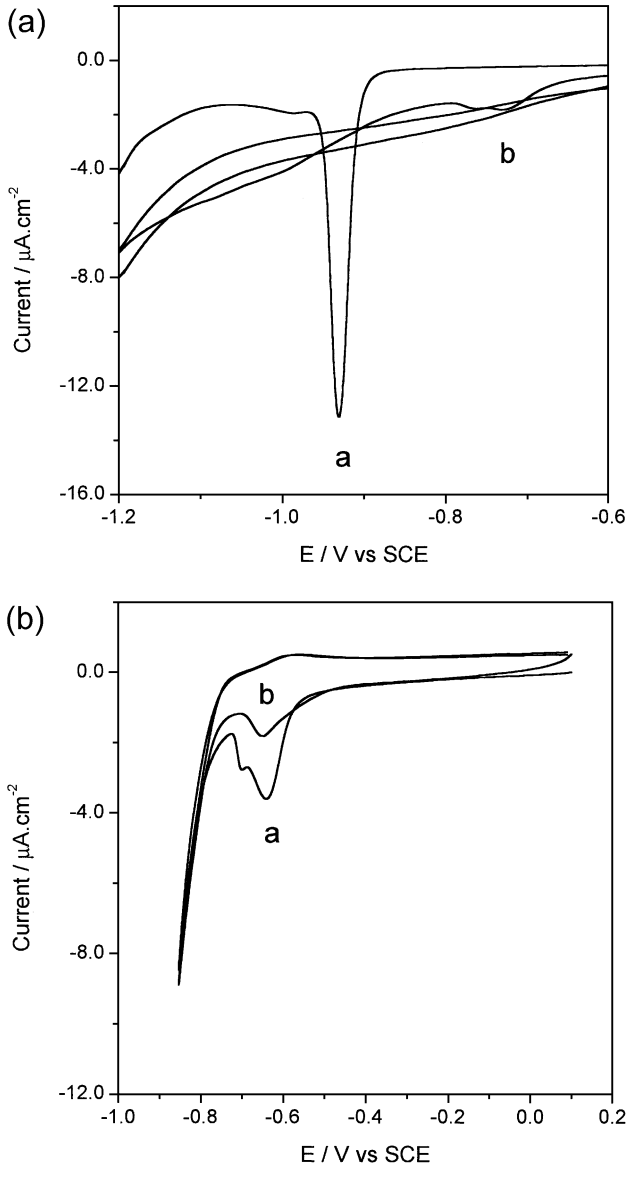

Fig. 3. Reductive desorption of the Gal*p* with thiol anchor **2** from Au(111). (a): 10 mM NaOH, pH 11.9; curve a: first scan; curve b: second scan. (b): 0.1 M phosphate buffer, pH 6.9; curve a: first scan; curve b: second scan; scan rate: 10 mV s^{-1}.

pH-dependent lateral interactions are indeed important. Insignificantly shifted but larger residual peaks are again apparent in the second scan (Fig. 3b), indicative of incomplete first scan desorption.

The peak potentials and coverages summarized in Table 1 show:

(a) Close to monolayer coverage is apparent at pH 11.9. The coverage is larger for molecule **3** than for molecule **2** due to the smaller size of the former.
(b) The coverages are significantly smaller at pH 6.9 than at pH 11.9, as noted due to incomplete adsorbate desorption in the first scans at pH 6.9.

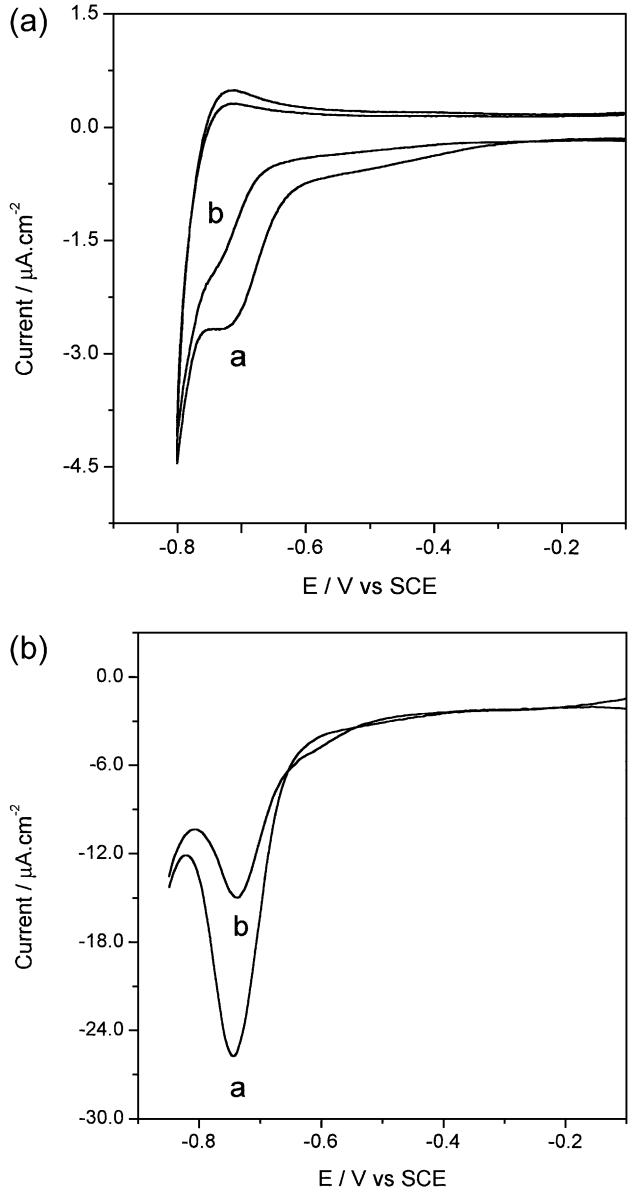

Fig. 4. Reductive desorption of the full 4-α-helix bundle carboprotein **1** from Au(111). 0.1 M phosphate buffer, pH 6.9. (a): Cyclic voltammetry; curve a: first scan; curve b: second scan. (b): Differential pulse voltammetry; curve a: first scan; curve b: second scan; scan rate: 10 mV s^{-1}.

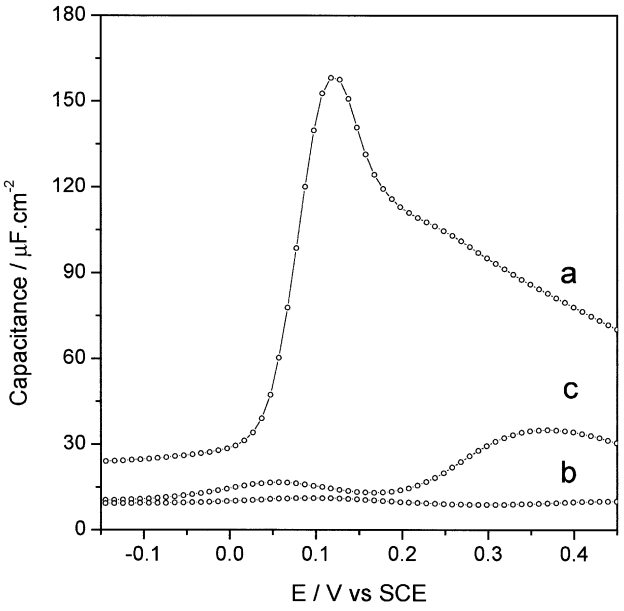

Fig. 5. Differential capacitance changes on adsorption of carboprotein **1** on Au(111) from 0.1 M phosphate buffer, pH 6.9. (a): Pure phosphate buffer. (b): After adsorption of carboprotein **1**. (c): After a single negative reduction potential excursion on carboprotein **1** adsorbed on Au(111).

Fig. 4a shows voltammetric scans of the carboprotein **1**, adsorbed on Au(111) in 0.1 M phosphate, pH 6.9. Reductive desorption at -707 mV on the ascending dihydrogen evolution wave is apparent. The adsorbate appears incompletely desorbed after a single scan. Differential pulse

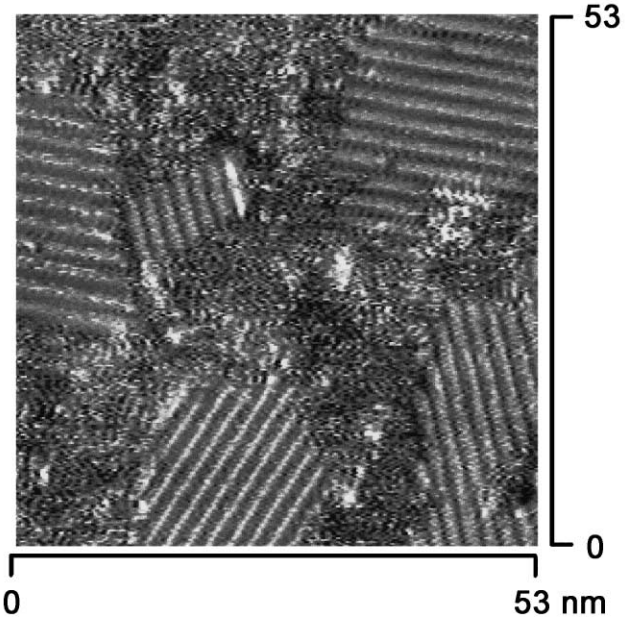

Fig. 6. In situ STM image of the thiol anchor molecule **3** showing domains of pin-striped organization of individual molecules, and domain boundaries. 0.1 M $HClO_4$ solution. Tunnelling current 0.3 nA. Bias voltage: 0.2 V. Substrate electrode potential: -0.8 V (vs. Pt-reference electrode).

voltammetry (Fig. 4b) shows a similar pattern. No desorption could be observed in 10 mM NaOH, where the carboprotein is rapidly degraded. Peak potentials and coverages according to a monolayer (Table 1) correspond to a significantly smaller number of molecules than for molecules **2** and **3** due to the larger size of the full carboprotein.

Fig. 5 shows differential capacitance changes on carboprotein adsorption and reductive desorption. A strong phosphate adsorption peak dominates in pure buffer [28]. This peak disappears on protein adsorption but partly reappears after a negative potential excursion. Fig. 6 shows, finally, an in situ STM image of molecule **3** on Au(111) in 0.1 M $HClO_4$. This investigation is preliminary, but the image shows clearly regular domains of adsorbed molecules. The combined data, based on linear voltammetry, capacitance measurements, in situ STM, and use of single-crystal electrodes show that controlled adsorption of biological molecules of systematically increasing complexity can be achieved. This holds promise for investigations of 4-α-helix bundle proteins with redox centres such as heme groups, inserted by axial histidine coordination in the helices [14,15,17], or noncovalently by the heme group preference for the hydrophobic interior between the helices.

Acknowledgements

Financial support from the Technical Science Research Council is acknowledged. The Alfred Benzon Foundation is acknowledged for a Bøje Benzon Fellowship to KJJ.

References

[1] T.A. Horbett, J.L. Brash (Eds.), Proteins at Interfaces: Part II. Fundamentals and Applications, ACS Symp. Ser., vol. 602, American Chemical Society, Washington, 1995.
[2] E. Katz, V. Heleg-Shabtai, A. Bardea, I. Willner, H.K. Rau, W. Haehnel, Fully integrated biocatalytic electrodes based on bioaffinity interactions, Biosens. Bioelectron. 13 (1998) 741–756.
[3] Q. Chi, J. Zhang, J.U. Nielsen, E.P. Friis, I. Chorkendorff, G.W. Canters, J.E.T. Andersen, J. Ulstrup, Molecular monolayers and interfacial electron transfer of *Pseudomonas Aeruginosa* azurin on Au(111), J. Am. Chem. Soc. 122 (2000) 4047–4055.
[4] D. Hobara, K. Niki, C.G. Zhou, G. Shumanov, T.M. Cotton, Characterization of cytochrome *c* immobilized on modified gold and silver electrodes by surface-enhanced Raman spectroscopy, Colloids Surf., A 93 (1994) 241–250.
[5] S. Lecomte, H. Wackerbarth, T. Soulimane, G. Buse, P. Hildebrandt, Time-resolved surface-enhanced resonance Raman spectroscopy for studying electron transfer dynamics of heme proteins, J. Am. Chem. Soc. 120 (1998) 7381–7382.
[6] L.H. Guo, H.A.O. Hill, Direct electrochemistry of proteins and enzymes, Adv. Inorg. Chem. 36 (1991) 341–375.
[7] F.A. Armstrong, H.A. Heering, J. Hurst, Reactions of complex metalloproteins studied by protein-film voltammetry, Chem. Soc. Rev. 26 (1997) 169–179.
[8] J.E.T. Andersen, P. Møller, M.V. Pedersen, J. Ulstrup, Cytochrome *c* dynamic at gold and glassy carbon electrodes monitored by in situ scanning tunnelling microscopy, Surf. Sci. 325 (1995) 193–205.
[9] J. Zhang, Q. Chi, S. Dong, E. Wang, In situ electrochemical scanning tunnelling microscopy investigation of structure for horseradish peroxidase and its electrocatalytic property, Bioelectrochem. Bioenerg. 39 (1996) 267–274.
[10] E.P. Friis, J.E.T. Andersen, L.L. Madsen, P. Møller, J. Ulstrup, In situ STM and AFM of the copper protein *Pseudomonas Aeruginosa* azurin, J. Electroanal. Chem. 431 (1997) 35–38.
[11] J.J. Davis, C.M. Halliwell, H.A.O. Hill, G.W. Canters, M.C. van Amsterdam, M.P. Verbeet, Protein adsorption at a gold electrode studied by in situ scanning tunnelling microscopy, New J. Chem. 22 (1998) 1119–1123.
[12] Q. Chi, J. Zhang, J.E.T. Andersen, J. Ulstrup, Ordered assembly and controlled electron transfer of the blue copper protein azurin at gold(111) single-crystal substrates, J. Phys. Chem. B 105 (2001) 4669–4679.
[13] W.F. DeGrado, C.M. Summa, V. Pavone, F. Nastri, A. Lombardi, De novo design and structural characterization of proteins and metalloproteins, Annu. Rev. Biochem. 68 (1999) 779–819.
[14] C.T. Choma, J.D. Lear, M.J. Nelson, P.L. Dutton, D.E. Robertson, W.F. DeGrado, Design of a heme-binding four-helix bundle, J. Am. Chem. Soc. 116 (1994) 856–865.
[15] D.E. Robertson, R.S. Farid, C.C. Moser, J.L. Urbauer, S.E. Mulholland, R. Pidikiti, J.D. Lear, A.J. Wand, W.F. DeGrado, P.L. Dutton, Design and synthesis of multi-haem proteins, Nature 368 (1994) 425–432.
[16] M. Mutter, S. Vuilleumier, A chemical approach to protein design—template-assembled synthetic proteins (TASP), Angew. Chem., Int. Ed. Engl. 28 (1989) 535–554.
[17] H.K. Rau, N. DeJonge, W. Haehnel, Combinatorial synthesis of four-helix bundle hemoproteins for tuning of cofactor properties, Angew. Chem., Int. Ed. 39 (2000) 250–253.
[18] K.J. Jensen, G. Barany, Carbopeptides: carbohydrates as potential templates for de novo design of protein models, J. Pept. Res. 56 (2000) 3–11.
[19] J. Brask, K.J. Jensen, Carbopeptides: chemoselective ligation of peptide aldehydes to an aminooxy-functionalized D-galactose template, J. Pept. Sci. 6 (2000) 290–299.
[20] J. Brask, K.J. Jensen, Carboproteins: a 4-α-helix bundle protein model assembled on a D-galactopyranoside template, Bioorg. Med. Chem. Lett. 11 (2001) 697–700.
[21] A. Avila, B.W. Gregory, K. Niki, T.M. Cotton, An electrochemical approach to investigate gated electron transfer using a physiological model system: cytochrome *c* immobilized on carboxylic acid-terminated alkanethiol self-assembled monolayers on gold electrodes, J. Phys. Chem. B 104 (2000) 2759–2766.
[22] Q. Chi, J. Zhang, E.P. Friis, J.E.T. Andersen, J. Ulstrup, Electrochemistry of self-assembled monolayers of the blue copper protein *Pseudomonas Aeruginosa* azurin on Au(111), Electrochem. Comm. 1 (1999) 91–96.
[23] J. Clavilier, R. Faure, G. Guinet, R. Durand, Preparation of monocrystalline Pt microelectrodes and electrochemical study of the plane surfaces cut in the direction of the (111) and (110) planes, J. Electroanal. Chem. 107 (1980) 205–209.
[24] A. Hamelin, Cyclic voltammetry at gold single-crystal surfaces: Part 1. Behaviour at low-index faces, J. Electroanal. Chem. 411 (1996) 1–11.
[25] G.E. Poirier, Characterization of organosulfur molecular monolayers on Au(111) using scanning tunneling microscopy, Chem. Rev. 97 (1997) 1117–1127.
[26] F. Schreiber, Structure and growth of self-assembling monolayers, Prog. Surf. Sci. 65 (2000) 151–256.
[27] J. Zhang, Q. Chi, J.U. Nielsen, E.P. Friis, J.E.T. Andersen, J. Ulstrup, Two-dimensional cysteine and cystine cluster networks on Au(111) disclosed by voltammetry and in situ scanning tunneling microscopy, Langmuir 16 (2000) 7229–7237.
[28] A. Cuesta, M. Kleinert, D.M. Kolb, The adsorption of sulphate and phosphate on Au(111) and Au(100) electrodes: an in situ STM study, Phys. Chem. Chem. Phys. 2 (2000) 5684–5690.